Supplementary Materials

Structure Boundary Preserving Segmentation for Medical Image with Ambiguous Boundary

Contents

A. Details of Network Structures

In Section 4. Experimental results, we conducted experiments with various segmentation network structures. This section describes a detailed segmentation network structures.

A.1 Segmentation Network

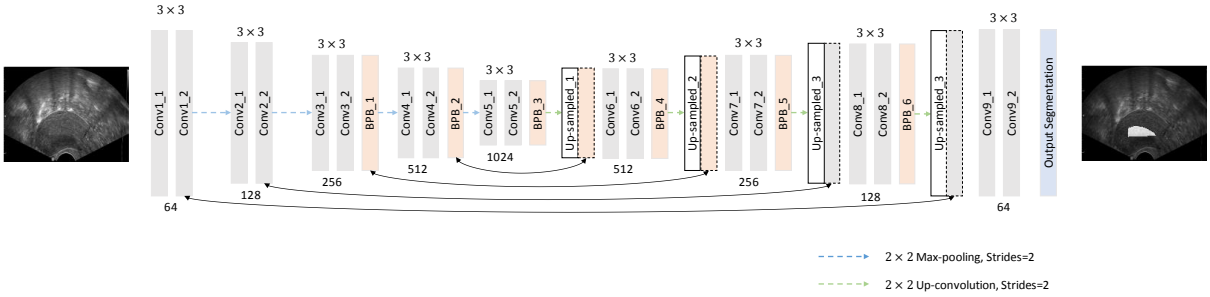

Fig. 6. The detailed structure of U-Net + BPB network.

First of all, we adopted our proposed Boundary Preserving Block (BPB) to U-Net. The U-Net has mirrored encoding (high-resolution to low-resolution) and decoding (low-resolution to high-resolution) structures. Skip-connection transfers encoding feature map to decoding feature maps of the same resolution. Initially, it integrated BPB after 6 convolution layers. Then, we adopted BPB prior to every max-pooling and up-convolution layer. Fig. 6 shows the detailed structure of U-Net + BPB network.

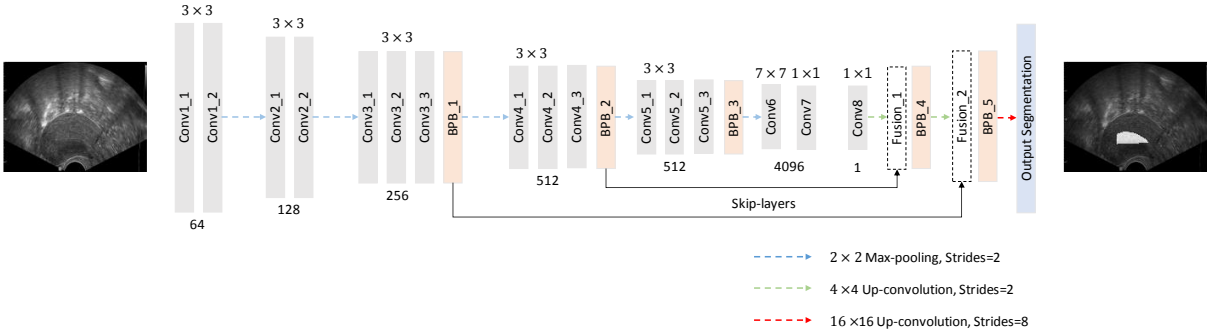

Fig. 7. The detailed structure of FCN + BPB network.

Secondly, we adopted our proposed BPB to FCN. The FCN uses skip-layers that fused semantic information from the deep, coarse layer with shallow, fine layer to produce detailed segmentation results. It also initially integrated BPB after 6 convolution layers. Then, BPB is implemented prior to every max-pooling and up-convolution layer. Fig. 7 shows the detailed structure of FCN + BPB network.

Lastly, we adopted our proposed BPB to Dilated-Net. The Dilated-Net consists of front -end network and context module. The front-end network structure is based on the FCN8s. Unlike FCN8s, the Dilated-Net used dilated convolution to enlarge the receptive fields effectively. In the front-end network, we adopted BPB after 7 convolution layers. Then, we adopted BPB prior to change the dilation rates in front-end network. In the context module, we adopted BPB prior to up-convolution. Fig. 8 shows the detailed structure of Dilated-Net + BPB network.

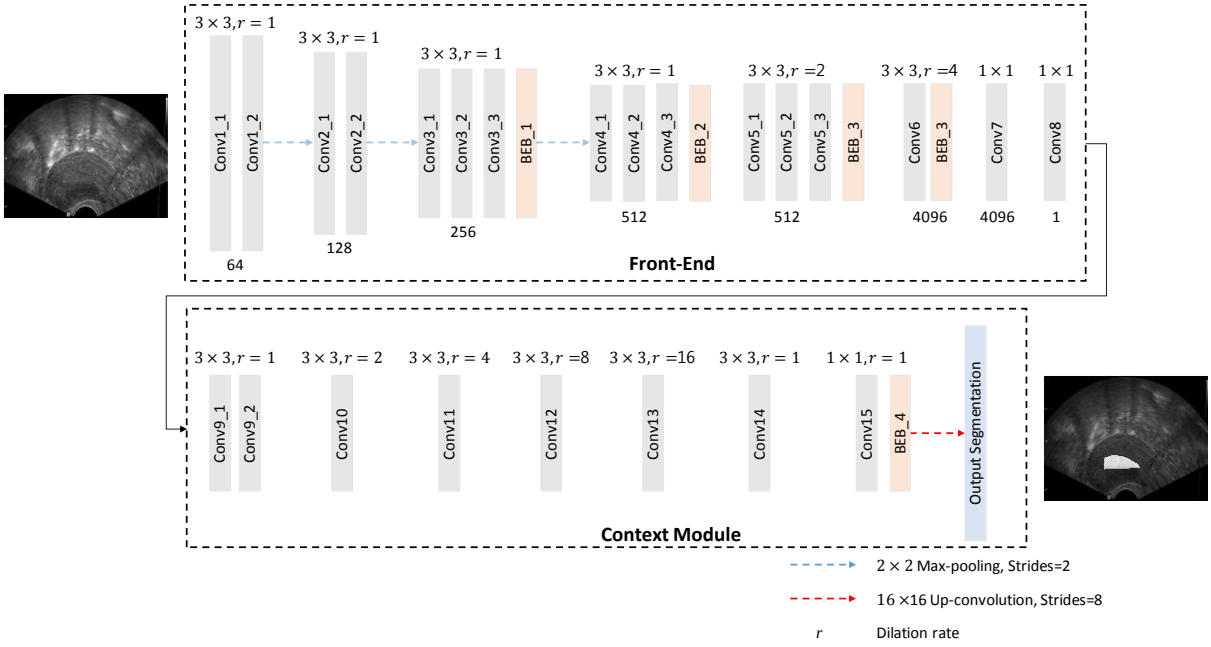

Fig. 8. The detail structure of Dilated-Net + BPB network.

A.2 Shape Boundary-aware Evaluator

In Section 3.2. Shape Boundary-aware Evaluator of the main paper, we described the Shape Boundary-aware Evaluator (SBE). This section describes the detailed SBE network structures. The inputs of SBE are segmentation map and boundary key-point map. They are concatenated and fed into SBE. Fig. 9 shows the detailed structure of SBE network.

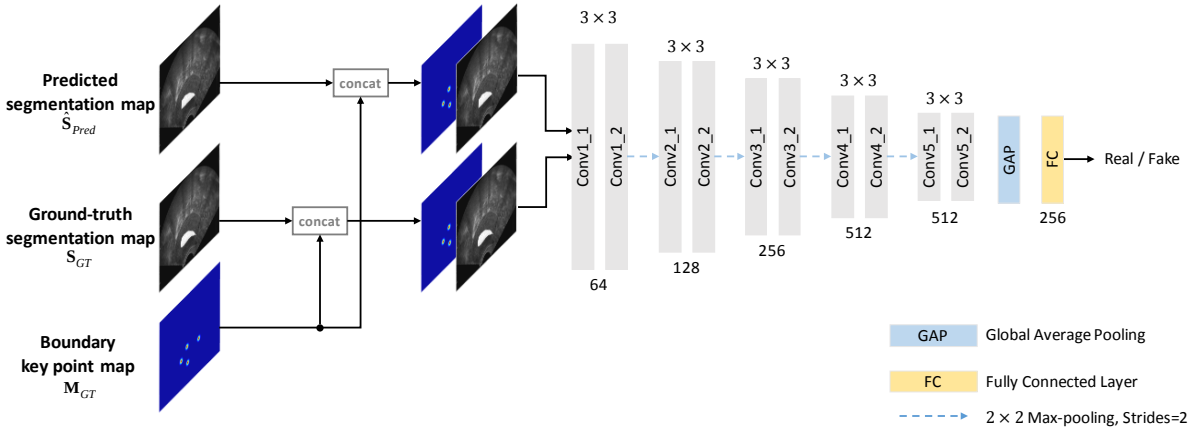

Fig. 9. The detail structure of Shape Boundary-aware Evaluator network.

B. More Qualitative Results with Various Segmentation Network

B.1 U-Net + BPB + SBE

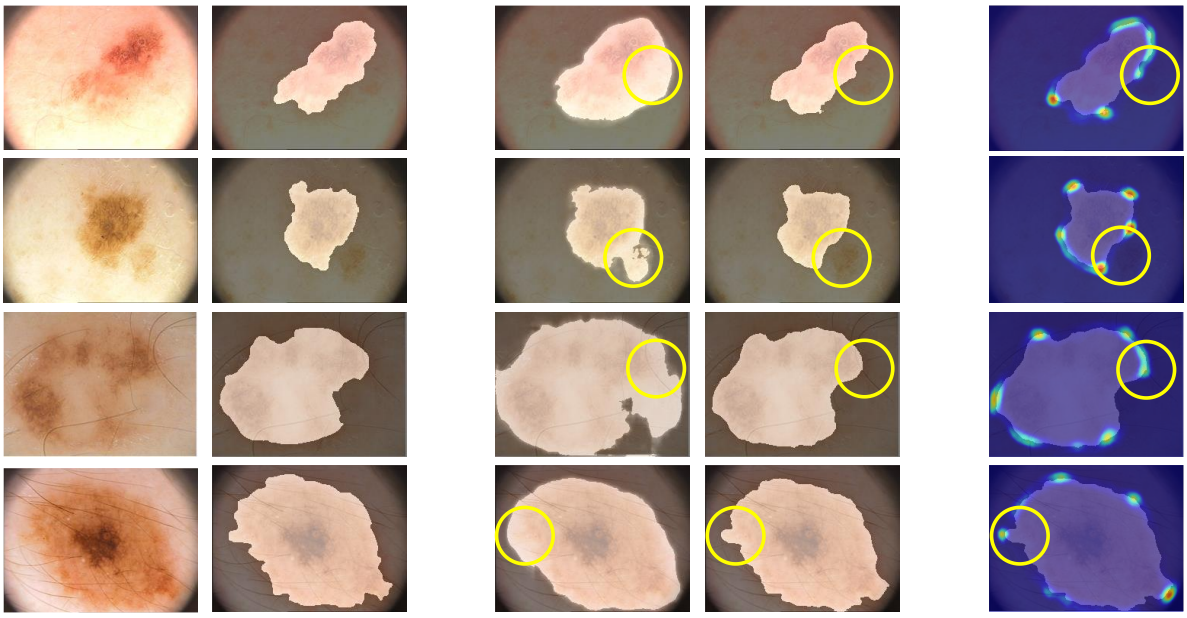

(a) Input (b) Ground Truth (c) U-Net (d) U-Net + BPB+SBE (e) Predicted Boundary Point Map

Fig. 10. Qualitative performance evaluation of the segmentation network on PH2+ISBI 2016 dataset. (a) is original input image and (b) is ground truth segmentation map. (c) is the segmentation results of U-Net and (d) is the segmentation results of U-Net + BPB + SBE network. (e) is the visualization of the boundary key point map of the last BPB.

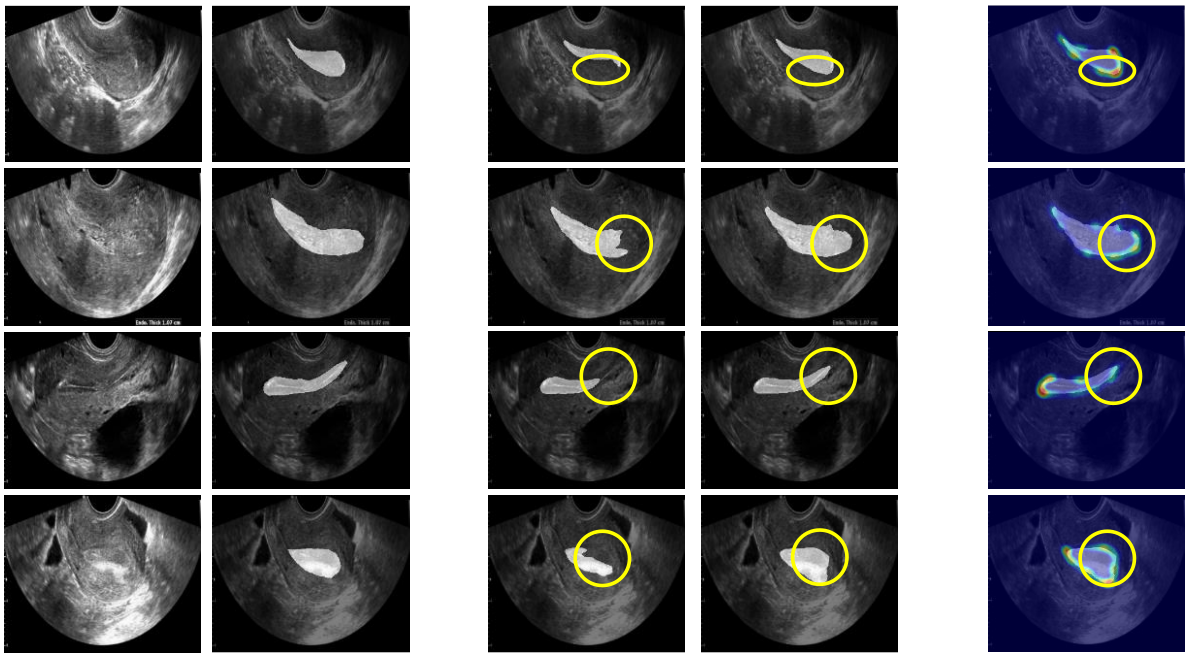

(a) Input (b) Ground Truth (c) U-Net (d) U-Net + BPB+SBE (e) Predicted Boundary Point Map

Fig. 11. Qualitative performance evaluation of the segmentation network on TVUS dataset. (a) is original input image and (b) is ground truth segmentation map. (c) is the segmentation results of U-Net and (d) is the segmentation results of U-Net + BPB + SBE network. (e) is the visualization of the boundary key point map of the last BPB.

B.2 FCN + BPB + SBE

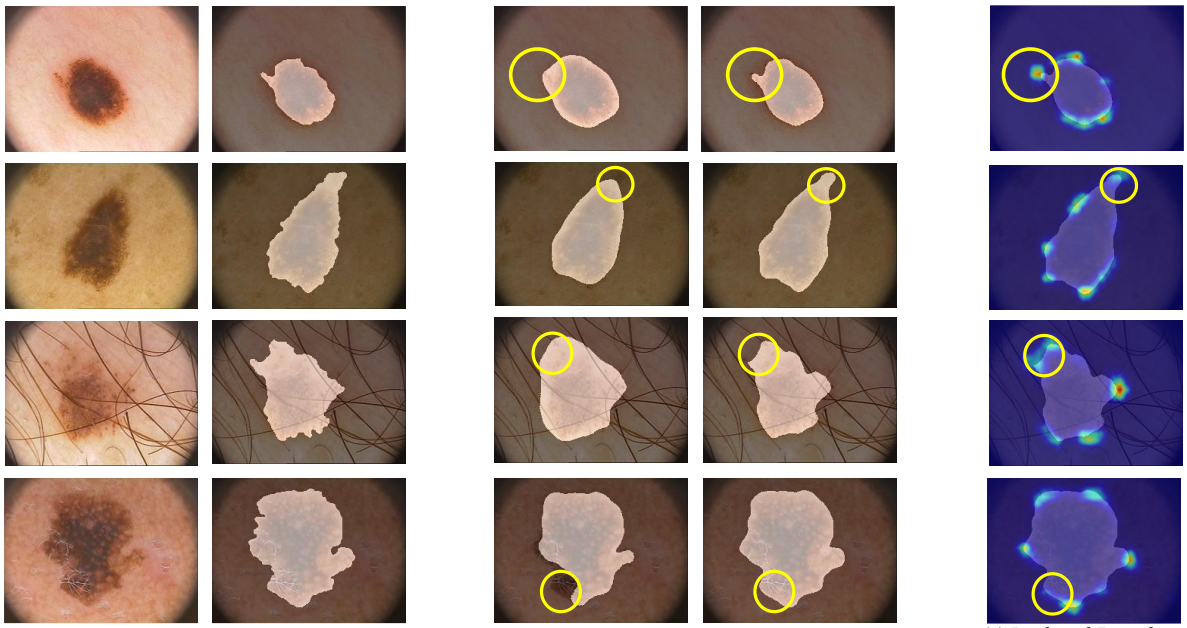

(a) Input (b) Ground Truth (c) FCN (d) FCN + BPB+SBE (e) Predicted Boundary Point Map

Fig. 12. Qualitative performance evaluation of the segmentation network on PH2+ISBI 2016 dataset. (a) is original input image and (b) is ground truth segmentation map. (c) is the segmentation results of FCN and (d) is the segmentation results of FCN + BPB + SBE network. (e) is the visualization of the boundary key point map of the last BPB.

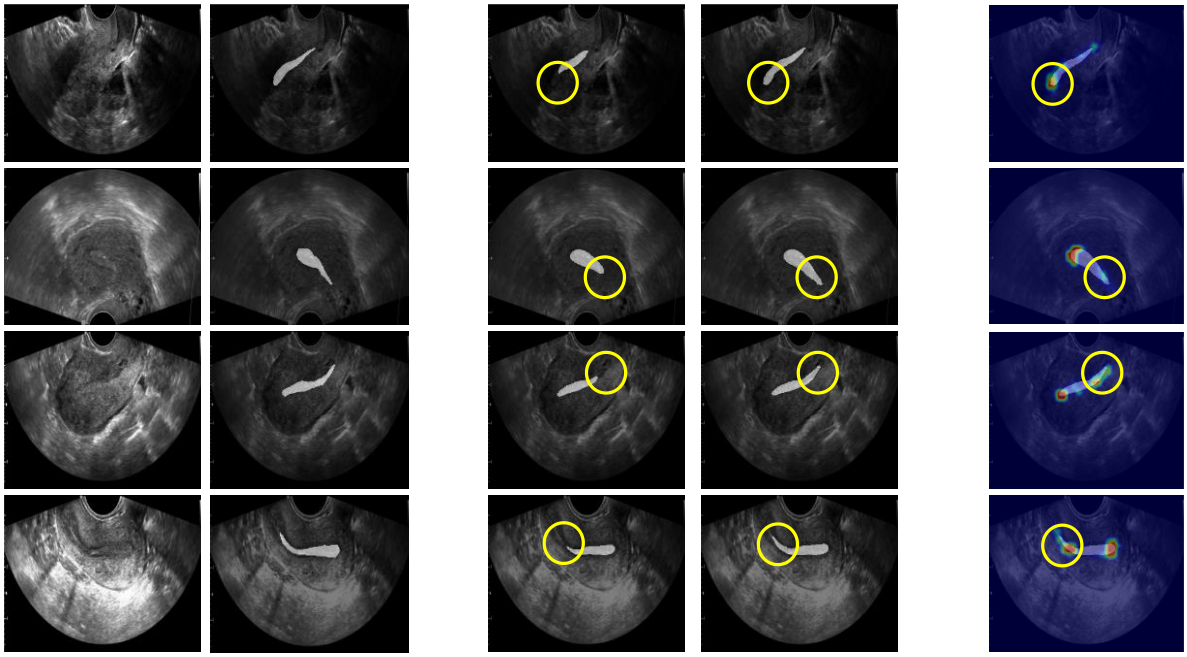

(a) Input (b) Ground Truth (c) FCN (d) FCN + BPB+SBE (e) Predicted Boundary Point Map

Fig. 13. Qualitative performance evaluation of the segmentation network on TVUS dataset. (a) is original input image and (b) is ground truth segmentation map. (c) is the segmentation results of FCN and (d) is the segmentation results of FCN + BPB + SBE network. (e) is the visualization of the boundary key point map of the last BPB.

B.3 Dilated-Net + BPB + SBE

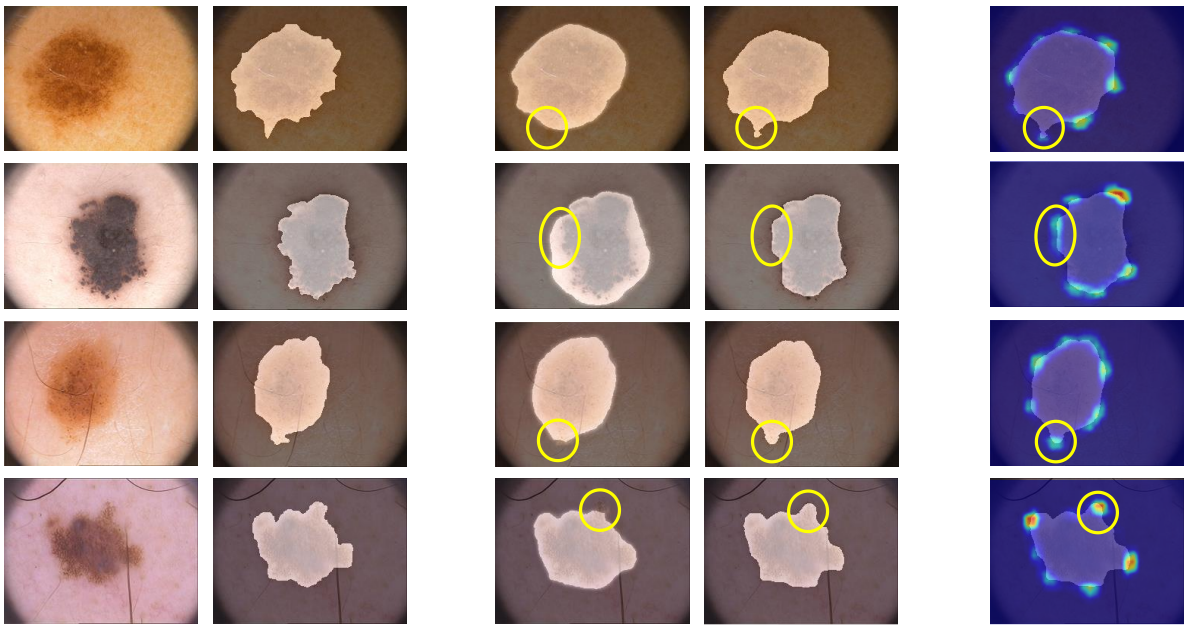

(a) Input (b) Ground Truth (c) Dilated-Net (d) Dilated-Net + BPB+SBE (e) Predicted Boundary Point Map

Fig. 14. Qualitative performance evaluation of the segmentation network on PH2+ISBI 2016 dataset. (a) is original input image and (b) is ground truth segmentation map. (c) is the segmentation results of Dilated-Net and (d) is the segmentation results of Dilated-Net + BPB + SBE network. (e) is the visualization of the boundary key point map of the last BPB.

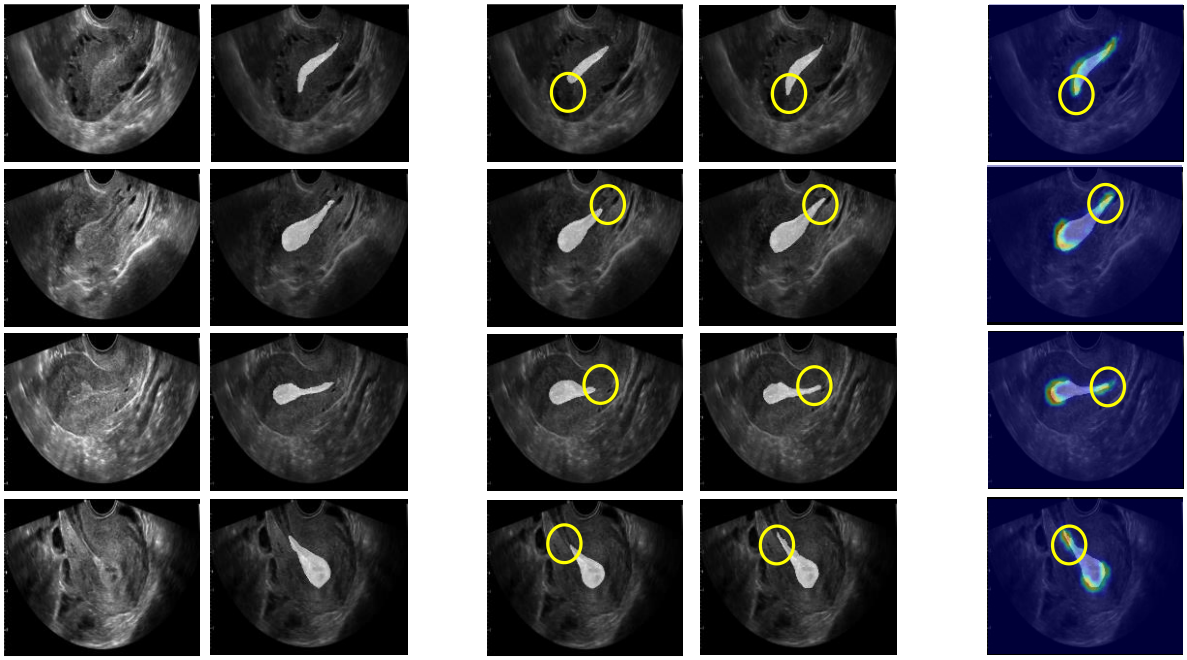

(a) Input (b) Ground Truth (c) Dilated-Net (d) Dilated-Net + BPB+SBE (e) Predicted Boundary Point Map

Fig. 15. Qualitative performance evaluation of the segmentation network on TVUS dataset. (a) is original input image and (b) is ground truth segmentation map. (c) is the segmentation results of Dilated-Net and (d) is the segmentation results of Dilated-Net + BPB + SBE network. (e) is the visualization of the boundary key point map of the last BPB.

C. Performance Evaluation in Accordance with the Number of Boundary Key Points

In this section, we report the performance evaluation in accordance with the number of boundary key points on Endometrium dataset. In the experiments, we evaluated the performance by changing the number of boundary key points to n=4,6,8,10. Fig. 16 shows the performance variation when the number of points changes for each network. In all networks, the best performance is given when n is 6, and the performance slightly changed depending on the number of points. Also, the results show that using BPB and SBE improves performance regardless of the number of points.

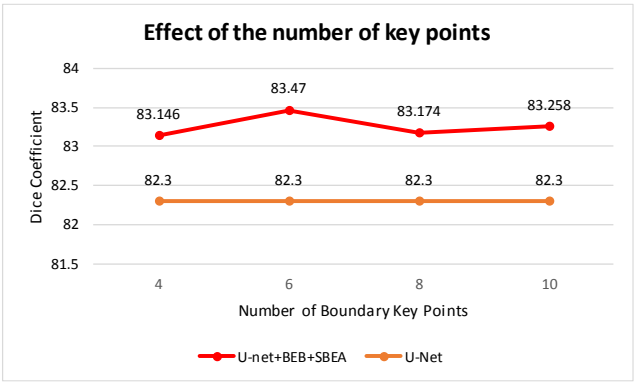

(a)

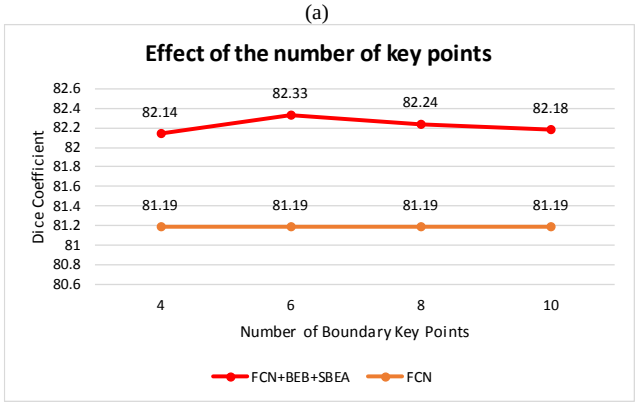

(b)

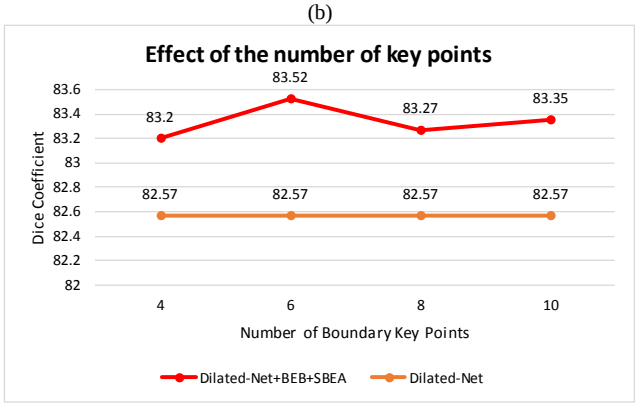

(c)

Fig. 16. Performance evaluation in accordance with the number of boundary key points on TVUS dataset. (a) is the results of U-Net and U-Net + BPB + SBEA. (b) is the results of FCN and FCN + BPB + SBEA. (c) is the results of Dilated-Net and Dilated-Net + BPB + SBEA.

D. Boundary Key Points Selection Results

In this section, we report the boundary key points selection results. The purpose of this experiment is to confirm that the results from the boundary key points selection algorithm have consistency. To this end, we conducted three independent selection trials (T=40000). Fig. 17 shows the results from the boundary key points selection algorithm. As shown in Fig. 17, all three independents trials show similar selection results.

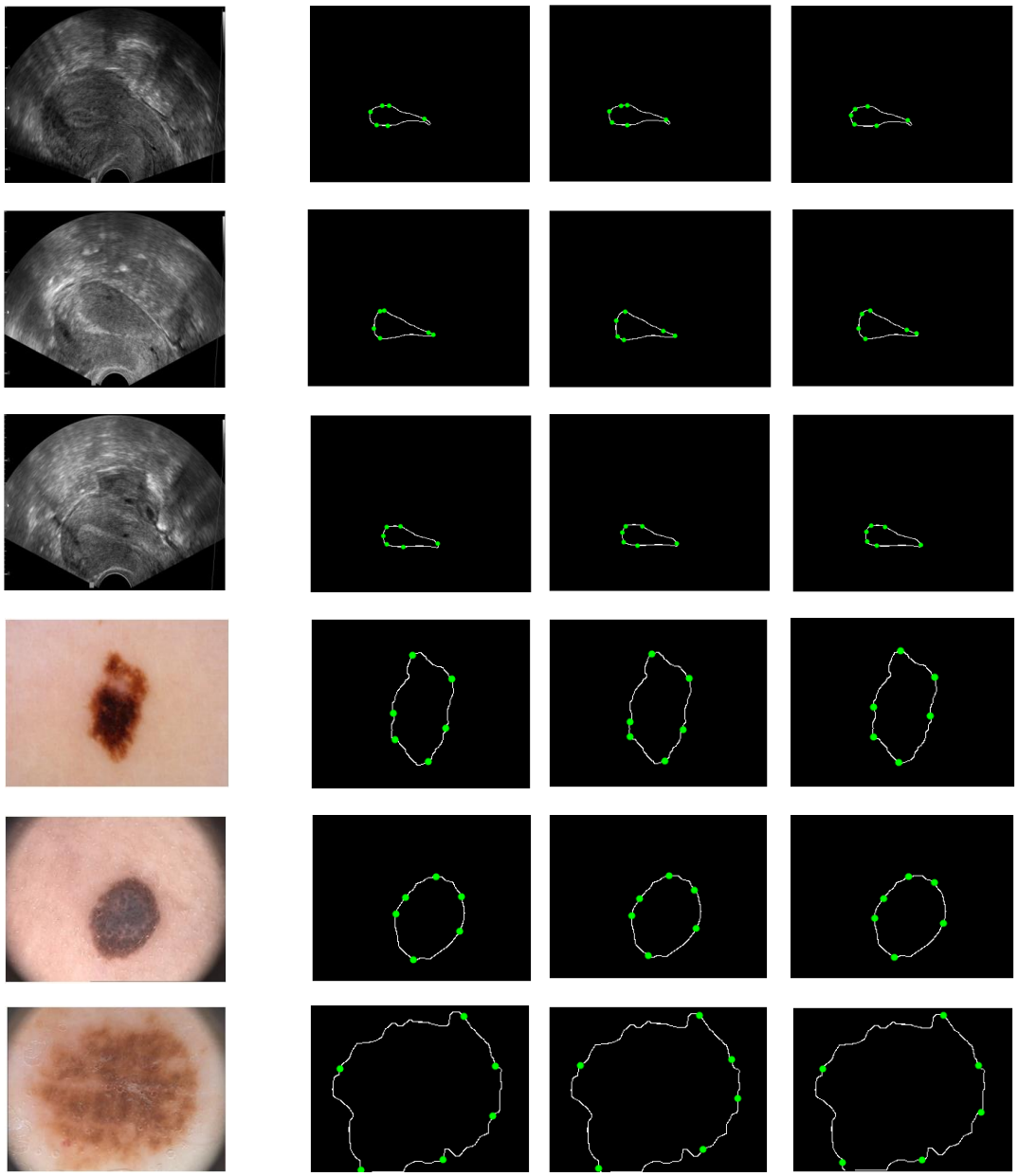

Fig. 17. Results from boundary key point selection algorithm. The first column is input images and second to fourth column are selected key points.

E. More Quantitative Results

Table 6. Qualitative experiment results comparison with loss based approaches.

	L_W	L_B	L_F	Proposed Method
PH2+ISBI 2016	90.01	90.33	89.73	90.65
TVUS	82.38	82.57	82.43	83.47

In this section, we further verify the effectiveness of the proposed method by comparing with loss-based approaches. We report three loss-based approaches (Weighted Loss (L_W) [R1], Boundary Loss (L_B) [R2], and Focal Loss (L_F) [R3]). We use U-Net as a backbone network and evaluate with Dice coefficient. Table 6 shows the experiment results on PH2+ISBI 2016 dataset and TVUS dataset.

On the PH2+ISBI 2016 dataset, each loss-based method shows L_W: 90.01%, L_B:90.33%, and L_F: 89.73%, respectively. Our method shows 90.65% on PH2+ISBI 2016 dataset. In particular, on the challenging TVUS dataset with fuzzy boundaries, our method shows 83.47%. On the other hand, each loss-based method shows L_W: 82.38%, L_B:82.57%, and L_F: 82.43%, respectively. Our proposed method shows superior performance when the boundaries are ambiguous.

Reference

[R1] Ronneberger, Olaf, Philipp Fischer, and Thomas Brox. "U-net: Convolutional networks for biomedical image segmentation." International Conference on Medical image computing and computer-assisted intervention. Springer, Cham, 2015.

[R2] Kervadec H, Bouchtiba J, Desrosiers C, et al. Boundary loss for highly unbalanced segmentation International Conference on Medical Imaging with Deep Learning. 2019: 285-296.

[R3] Lin, Tsung-Yi, et al. "Focal loss for dense object detection." Proceedings of the IEEE international conference on computer vision. 2017.